Available online at www.joac.info

ISSN: 2278-1862

Journal of Applicable Chemistry

2015, 4 (3): 857-864

(International Peer Reviewed Journal)

Synthesis and Characterization of Copper and Tin Codoped TiO_2 Nanoparticles

P. Babji* and I. Nageswara Rao

*Department of Physical, Nuclear Chemistry & Chemical Oceanography,
School of Chemistry, Andhra University, Visakhapatnam 530 003, Andhra Pradesh, **INDIA**

Email: babjichemistry007@gmail.com

Accepted on 29th April 2015

ABSTRACT

Copper and tin co-doped Titania nanophotocatalyst has been prepared by Sol gel method and characterized by XRD, FE-SEM, EDS, FT-IR, HR-TEM and SAED. X-ray diffraction studies of the Cu^{2+}-Sn^{4+}/TiO_2 show the presence of anatase phase TiO_2 and in the sample prepared from 0.05, 0.10, 0.15 and 0.20 mmol have also shown the presence of anatase phase only in which 0.15mmol of Cu^{2+}-Sn^{4+}/TiO_2 is the optimum concentration. The FE-SEM images of the prepared samples showed the decrease in size and morphological change of the TiO_2 particles when compared to un-doped TiO_2. The presence of elements copper, tin, titanium and oxygen were confirmed by Energy Dispersed Spectroscopy (EDS). From TEM images it can be concluded that the addition of dopants to titania hinders the growth of nanoparticles. These results suggested that the simple and cost effective method and shows excellent adsorption removal properties on dyes for industrial applications.

Keywords: copper and tin co-doped TiO_2, Sol-gel.

INTRODUCTION

Large amounts of coloured waste water are generated in industries which use dyes to impart a desired colour to their products (food, paper, rubber, textile, plastics), and are discharged into natural hydric bodies with undesirable consequences to the environment and to human health [1–4]. The potential way to utilize these properties in various applications could be to integrate graphene sheets in composite materials such as in the preparation of highly photoactive composites materials based on TiO_2 and ZnO [5]. Nanomaterials usage is continuously being increased rapidly and widely in areas such as cosmetics, eatables, pharmaceuticals and other industrial applications. [6].

The most widely studied catalyst in this respect is TiO_2 in view of its favorable physicochemical properties, low cost, easy availability, high stability, and low toxicity [7]. However, it is active only in the UV range which constitutes less than 5% of sunlight. Photocatalytic reactions take place when particles of the semiconductor absorb photon of energy equal to or greater than its band gap and the electrons get excited from the valence band to the conduction band. This results in the formation of an electron-hole pair which promotes oxidation/reduction of the adsorbed substrate. In aqueous solution, the reactive OH

radicals can promote the oxidation and eventual mineralization of organic compounds. The photocatalytic activity of TiO_2 nanoparticles under ultraviolet light particularly is prominent in the anatase form, but it has been recently found that this oxide, when doped with nitrogen ions, is also a photocatalyst under visible light [8].

Sol-gel process is one of the versatile, simple, and easy means of synthesizing nanosize materials in contrast to the other conventional preparation methods which do not usually produce homogeneous, high-surface-area materials. The main advantage of the sol-gel method in preparing catalytic materials is its excellent control over the properties of the product via a host of parameters that are accessible in all four key processing steps: formation of a gel, aging, drying, and heat treatment. Although titania catalysts have been extensively studied, the procedure of preparing photocatalytic metal-doped titania is still of great interest. Particle size of catalyst is considered one of the most important physical parameters in these reactions, because it can directly furnish the active sites for the reaction to occur [9-11]. The prepared Cu^{2+} and Sn^{4+} co-doped TiO_2 photocatalyst was characterized by several analytical techniques such as XRD, FTIR, FE-SEM, EDS, HR-TEM and SAED.

MATERIALS AND METHODS

Copper Nitrate and Tin Chloride sources for preparing Cu^{2+} and Sn^{4+} co-doped TiO_2 photocatalysts and Titanium tetra-n-butoxide [$Ti(O\text{-}Bu)_4$] purchased from Merck, China and anhydrous ethanol were obtained from Hangzhou High-crystal Fine Chemical Co., Ltd., China.

Preparation of Copper and Tin co-doped TiO_2 nanoparticles: In brief, 0.02 mol tetrabutyl orthotitanate were added drop wise into 50 ml absolute ethanol to give a solution which was then vigorously stirred for 20 min at room temperature and add 3 drops of Conc. HNO_3. The desired amounts 0.05, 0.10, 0.15 and 0.20 mmol of copper nitrate and Tin Chloride (the molar ratio of Cu to Sn was 1:1) were then added in the reaction mixture while stirring continuously for 60 min until the Cu and Sn dopants were dissolved. An amount of 2.0 mL of deionized water was then dropped into the above solution. Afterwards, the resultant solution mixture was maintained at room temperature with continuous stirring for 2 h to form a gel which was then aged for 12 h at room temperature. After being dried at 80 ◦C for 24 h were obtained and then annealed at 400 ˚C for 3 h to give a light greenish material. An un-doped TiO_2 (anatase) sample was also prepared by adopting the above procedure without adding the Copper Nitrate and Tin Chloride which is pure TiO_2. The doping concentrations are expressed as mmol of titanium atom.

Characterization of $Cu^{2+}$and Sn^{4+}codoped TiO_2 nanoparticles: The FE-SEM micrographs were obtained by using a JEOL 6335F FE-SEM microscope equipped with a Thermo Noran energy dispersive spectroscopy (EDS) detector. The presence of elemental copper, tin, titanium and oxygen was confirmed through EDAX. The EDAX observations were carried out in STIC, CUSAT, (JOEL Model JED-2300). Crystalline structure and crystallinity were identified by X-ray diffraction (XRD, DX2700, China) operating with Cu Ka radiation (l ¼ 1.5418 ˚A) at a scan rate (2 θ) of 2˚ min^{-1} with the accelerating voltage of 40 kV and the applied current of 45 mA, ranging from 5˚ to 80˚. Fourier transform infrared (FT-IR) spectra for Cu^{2+} and Sn^{4+} nanoparticles was obtained in the range 4,000 to 400 cm^{-1} with an IR-Prestige-21 Shimadzu FT-IR spectrophotometer, by KBr pellet method. The particle size and morphology of the sample and the corresponding selected area electron diffraction (SAED) were examined by high resolution transmission electron microscopy (HR-TEM) with an accelerating voltage of 200 kV, respectively.

RESULTS AND DISCUSSION

X-ray Diffraction Studies: Fig. 1.shows the XRD patterns of un-doped TiO_2 (curve a), 0.05 mmol Cu-Sn/TiO_2 (curve b), 0.10 mmol Cu-Sn/TiO_2 (curve c), 0.15 mmol Cu-Sn/TiO_2 (curve d) and 0.20 mmol Cu-Sn/TiO_2 (curve e) powders. It is found that the majority of the crystal phase is anatase for all of the

samples [12]. No diffraction peak corresponding to Cu and Sn was detected. The reason could be due to the fact that the content of Cu and Sn might be too small to detect. The inset in fig. 1 is the enlarged XRD peaks of crystal plane (101) for all of the samples.

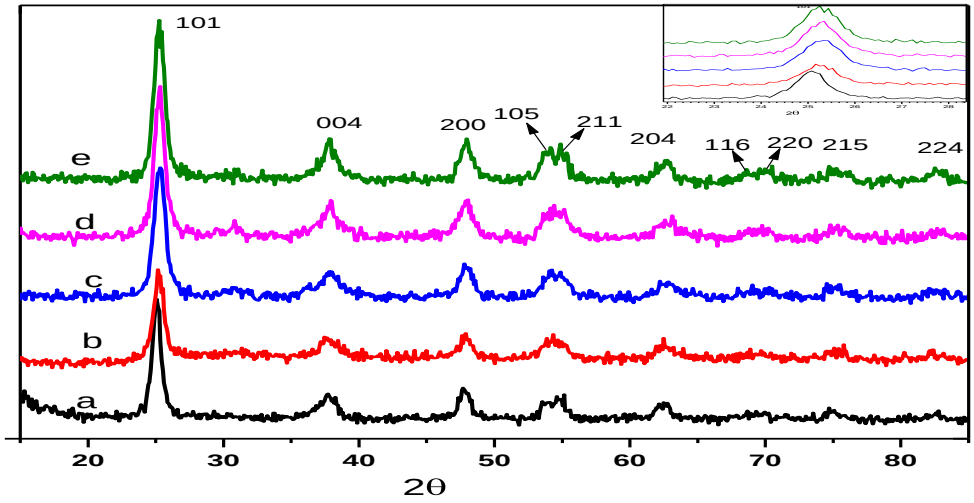

Fig. 1: XRD patterns of (a) Un-doped TiO_2, (b) 0.05, (c) 0.10, (d) 0.15 and (e) 0.20 mmol of Cu^{2+}-Sn^{4+}/TiO_2 nanoparticles. Inset is the enlarged XRD peaks of crystal plane (101).

Compared with the un-doped TiO_2, peak shift of the peak position is observed. The intensity of anatase TiO_2 peaks increased due to doping, and peaks corresponding to $CuNO_3$ and $SnCl_4$ were not detected. This may be due to the well dispersion of Cu^{2+} and Sn^{4+} content in TiO_2 particles. The well-defined diffraction peaks with 2θ are at about 25°, 38°, 48°, 54°, 54°, 62°, 68°, 70°, 74°, and 82° which are assigned to the (101), (004), (200), (105), (211), (204) (116), (220), (215) and (224) crystal planes, respectively. This XRD characteristic pattern is consistent with the standard JCPDS values of anatase TiO_2 (JCPDS Card No. 21-1272) [13-14] and did not appear in rutile and brookite form.

With increasing amount of Sn^{4+} there is a gradual diminishing of crystallites in all three phases. Concerned the structural properties, the very similar ionic radius of Ti^{4+} (0.605 Å) [15] and Sn^{4+} (0.690 Å) [16] would allow easy substitution of Ti^{4+} by Sn^{4+} in the TiO_2 lattice, in comparison to Sn^{2+} that is much larger, 1.22 Å [17]. Therefore, Sn^{2+} can only occupy the interstitial sites in [TiO_4] and [TiO_6], resulting in a decrease in the lattice distortion energy, while Sn^{4+} can substitute for Ti^{4+} in [TiO_4] and [TiO_6], resulting in an increase in the distortion energy [18].

Decrease in the particle size of TiO_2 might be ascribed to a broadening effect due to incorporation of the metal oxides into TiO_2 matrix [19], as can be seen by comparing the (101) reflection plane of pure TiO_2 with Cu-Sn/TiO_2 (Fig. 1). Moreover, the (101) reflection plane of the Cu-Sn/TiO_2 samples shifted to higher diffraction angle relative to pure TiO_2 (Fig. 1(Inset)), implying an incorporation effect of copper at the TiO_2 lattice as Ti^{4+} position may be substituted by copper due to the similarity of their ionic radii (Ti=0.68 Å and Cu = 0.72 Å) [20].

Field Emission-Scanning Electron Microscopic study: Field Emission Scanning Electron Microscopy was used to characterize the surface morphology and size of the particles. The surface morphology of the sample calcined at 400 °C corresponded to a mixture of nanoparticles (Fig. 2).

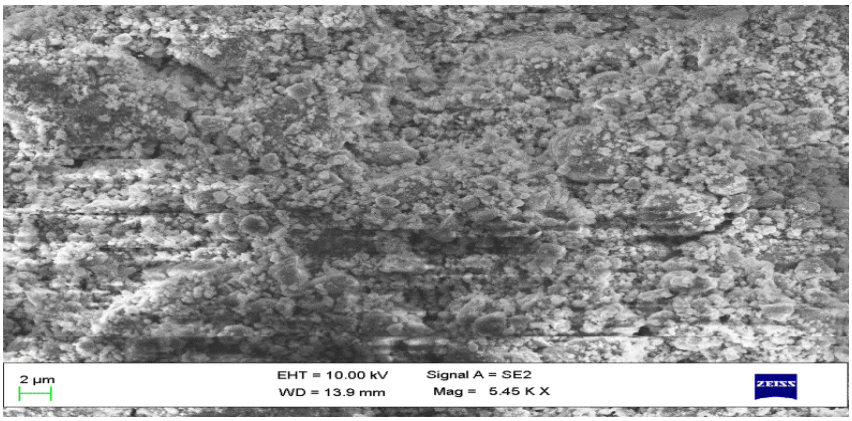

Fig. 2: FE-SEM image of 0.15 mmol Cu^{2+}-Sn^{4+}/TiO_2 nanoparticles.

The average particle size was ~30 nm. The morphology, structure and particle size of the powder were also further investigated by transmission electron microscopy.

Fourier Transform Infrared Spectroscopy Study: The FTIR spectra of the samples in the frequency range of 400–4000 cm^{-1} are shown in fig. 3. Furthermore, the broadening of ~3400 cm^{-1} O-H stretching vibration the formation of a different -OH group, and most probably as Ti-OH surface group. The broad intense band in the range of 450–700 cm^{-1} is due to the Ti–O stretching and Ti–O–Ti bridging stretching modes [21-24].

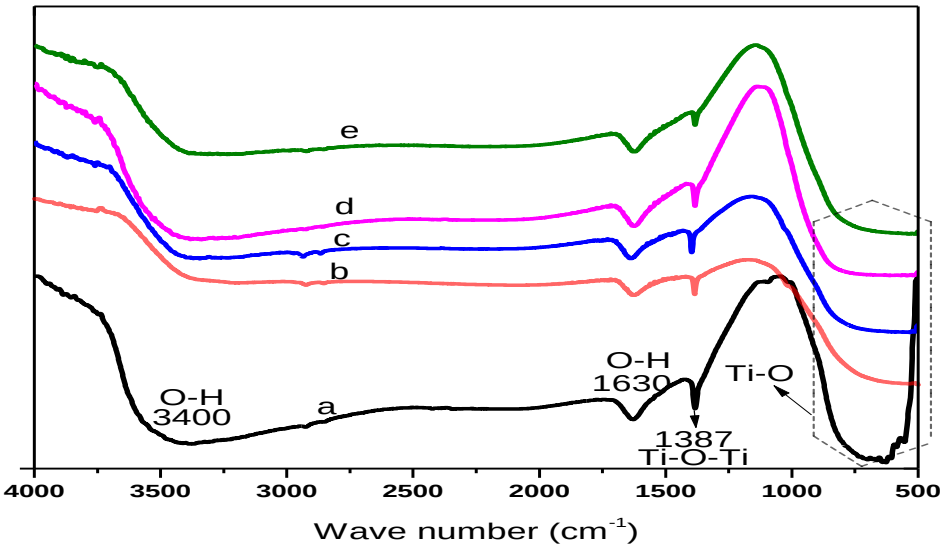

Fig. 3: FT-IR spectra of (a) Un-doped TiO_2, (b) 0.05, (c) 0.10, (d) 0.15 and (e) 0.20 mmol of Cu^{2+}-Sn^{4+}/TiO_2 nanoparticles.

The broad absorption peaks at about 3400 cm^{-1} and the band at 1625 cm^{-1} correspondto the surface adsorbed water and the hydroxyl groups [25]. Since the Ti–O bond is shorter than the Sn–O bond, the doping of Sn^{4+} in TiO_2 may lead to a shift of the lower wave number of Ti–O lattice vibration [26]. Copper and tin co-doped TiO_2 intensity has reduced compared to un-doped TiO_2. No additional peaks are present

upon Cu and Sn doping, supporting the efficient dispersion of copper and tin, and it indicates the absence of clusters of copper and tin, which is in good agreement with the XRD analysis result.

Energy Dispersive X-ray (EDX) spectra: The energy dispersive X-ray (EDX) spectra of cu and sn co-doped TiO_2 are shown in fig. 4, respectively. The peaks corresponding to titanium, oxygen and the respective doped metals copper and tin can be clearly seen in these spectra.

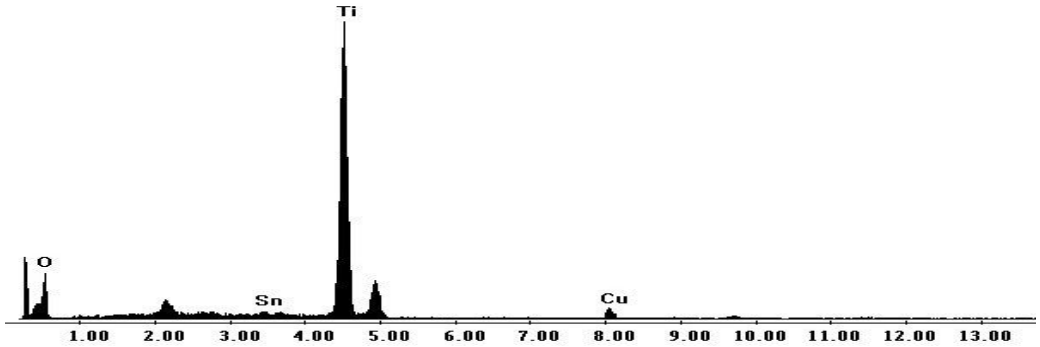

Fig. 4: EDS spectra of 0.15 mmol Cu^{2+}-Sn^{4+}/TiO_2 . nanoparticles.

Transmission Electron Microscopy: Transmission electron microscopy was used to examine the particle size, crystallinity and morphology of the samples.

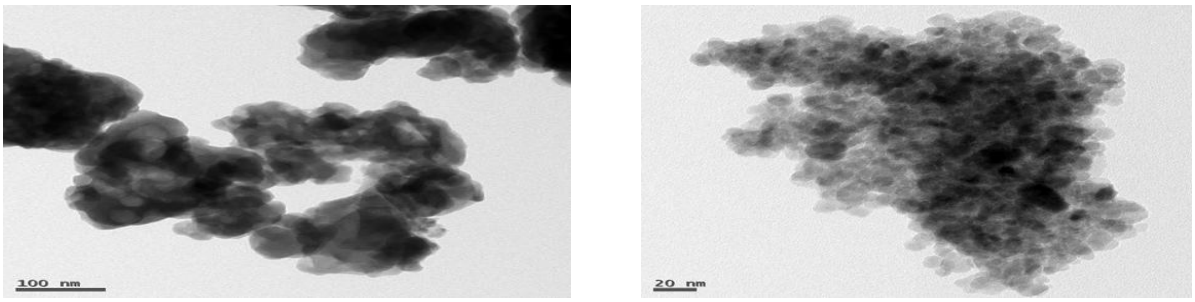

a) b)

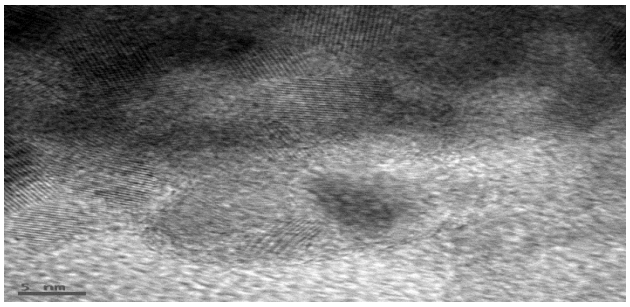

Fig. 5: TEM images of (a) Undoped TiO_2, (b) 0.15 mmol of Cu^{2+}-Sn^{4+}/TiO_2 nanoparticles, (c) HRTEM images of Cu^{2+}- Sn^{4+}/TiO_2 nanoparticles.

The main purpose of TEM is to characterize the object individually, not in the bulk. Fig. 5b shows the bright-field TEM image revealing the high resolution morphology of the nanostructured particles containing anatase TiO_2 calcined at 400 °C. It was observed that the titania was almost exclusively composed of small sized nanocrystallites. The anatase TiO_2 powder mostly had a spherical morphology.

High-resolution transmission electron microscopy (HR-TEM) was used to elucidate the surface planes of the titanium dioxide particles. Fig. 5c shows the discrete apparent crystallites. The clearly distributed anatase lattice fringe indicates that the titania was highly crystalline. The fringes of the TiO_2 nanocrystallites were used to determine the crystallographic spacing's and their orientation. Anatase nanocrystallites consisting of tetragonal particles with (101) plane surfaces were observed by HR-TEM [27]. The TiO_2 nanocrystals had many crystal lattice planes with a d spacing of 0.35 nm being obtained for the (101) plane. The fringes corresponding to the (101) crystallographic planes of anatase were the most prominent.

The particle size was close to 10 to 30 nm, with the observed sizes of the crystallites comparable to those calculated from the XRD patterns. Thus, the presence of nano sized particles was confirmed from the TEM images. The selected area electron diffraction (SAED, Fig. 6) pattern showed distinct and good diffraction rings corresponding to the anatase phase [27]. The intensity of the diffraction rings obtained from the particles indicated the crystalline nature of the particles, with a narrow particle size distribution.

Selected Area Electron Diffraction: Fig. 6. shows the crystallinity of titania was confirmed by the SAED pattern of copper and tin co-doped TiO_2 nanoparticles.

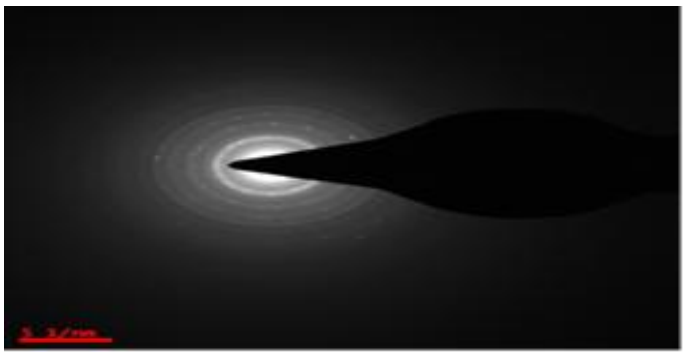

Fig. 6: SAED images of 0.15 mmol of Cu^{2+}-Sn^{4+}/TiO_2 nanoparticles.

The SAED pattern showed distinct and good diffraction rings corresponding to the anatase phase [28]. It shows well resolved bright and intense polymorphic ring patterns without any additional spots or rings of second phases. It revealed the typical diffraction rings for a crystalline powder, due to the absence of an amorphous nature. Image processing analysis of TEM micrographs is a useful method of fine-tuning the microstructure. It can be indexed to the reflection of Tetragonal structure in crystallography, and this result was also investigated by means of X-ray diffraction.

APPLICATIONS

The prepared Cu and Sn co-doped TiO_2 nanocoparticles by Sol-gel method. X-ray diffraction studies of the Cu^{2+}-Sn^{4+}/TiO_2 show the presence of anatase phase TiO_2 and in the sample preparation of 0.05, 0.10, 0.15 and 0.20 mmol have also shown the presence of anatase phase only. The FE-SEM images of the prepared samples showed the decrease in size and morphological change of the TiO_2 particles. These results suggested that the simple and cost effective method and shows excellent adsorption removal properties on dyes for industrial applications.

CONCLUSIONS

We synthesized a sol gel method for preparation of high quality of different concentrations of Cu and Sn co-doped TiO_2 with pure anatase phase using copper nitrate and tin chloride as Cu and Sn source. By

tuning the starting molar ratio of Cu and Sn to titanium, different doping level samples were obtained in which 0.15mmol of Cu^{2+}-Sn^{4+}/TiO_2 is optimum concentration. The nanophotocatalyst was characterized using XRD, FT-IR, FE-SEM, EDS, HR-TEM and SAED. The results showed that, the product was in the form of anatase phase. These results suggested that the simple and cost effective method and shows excellent adsorption removal properties on dyes for industrial applications.

ACKNOWLEDGMENTS

The author is thankful to UGC-BSR, New Delhi for financial support. The author is also thankful to University of Hyderabad for providing spectral data.

REFERENCES

[1] H. Zollinger, Color Chemistry: Synthesis, Properties and Applications of Organic Dyes and Pigments, Wiley-VCH, **1991**.
[2] Y. Bulut, H. Aydin, *Desalination.* **2006**, 194, 259–267.
[3] E.J. Weber, V.C. Stickney, *Water Research.* **1993**, 27, 63–67.
[4] C. Rafols, D. Barcelo, *Journal of Chromatography A.* **1997**, 777, 177–192.
[5] P. Suresh, U.S. Kumari, A.V. Prasada Rao, *J. Applicable. Chem.*, **2013**, 2 (6), 1627-1633.
[6] Shailesh Sharma1, Deepak Sinha, D. K. Sharma, Reena Nashine, *J. Applicable. Chem.* **2013**, 2 (5), 1244-1248.
[7] G. Parasuram Naidu, P. Suresh, R. Balaji Anjanayulu, A. Appalaraju, R. Murali Krishna. *J. Applicable. Chem,* **2014**, 3 (5), 2076-2083.
[8] T. Ihara, M. Miyoshi, Y. Iriama, O. Matumoto, S. Sugihara, *Appl. Catalysis B: Environ*, **2003**, 42, 403-409.
[9] C.H. Cho, D.K. Kim, D.H. Kim, *J. Am. Ceram. Soc*, **2003**, 86, 1138-1145.
[10] Y. Oguri, R. Riman, H.K. Bowen, *J. Mater. Sci,* **1988**, 90, 2897-2904.
[11] J.L. Look, C.F. Zukoski, *J. Am. Ceram. Soc*, **1992**, 75, 1587-1595.
[12] B.F. Gao, Y. Ma, Y.A. Cao, W.S. Yang, J.N. Yao, *J. Phys. Chem, B.* **2006**, 110, 14391.
[13] Y. Masuda, K. Kato, *Ceram. Soc. Jpn,* **2009**, 117, 373-376.
[14] L. Ge, M. Xu, M. Sun, H. Fang, *J. Sol-Gel Sci. Techn,***2006**, 38, 47-53.
[15] R.C. Pullar, S.J. Penn, X.Wang, I.M. Reaney, N.M. Alford, *J. Eur. Ceram. Soc,* **2009**, 29, 419-424.
[16] S. Wu, G. Wang, S. Wang, D. Liu, *J. Mater. Sci. Technol,* **2005**, 21, 773-775.
[17] H. Cox, A.J. Stace, *J. Am. Chem. Soc,* **2004**, 126, 3939-3947.
[18] Z.M. Shi, L. Yan, L.N. Jin, X.M. Lu, G.Zhao, *J. Non-Cryst. Solids,* **2007**, 353, 2171-2178.
[19] O. V´azquez-Cuchillo, A. Cruz-L´opez, L.M. Bautista Carrillo, A. Bautista-Hern,´andez, L.M. Torres Mart´ınez, S.W. Lee, *Res. Chem. Intermedie,* **2010**, 36, 103-113.
[20] R. L´opez, R. G´omez, M.E. Llanos, *Catal. Today*, **2009**, 148, 103-108.
[21] N. Venkatachalam, M. Palanichamy, B. Arabindoo, V. Murugesan, *J. Mol. Catal. A: Chem*, **2007**, 266, 158-165.
[22] X. Chen, X. Wang, X. Fu, *Energy Environ. Sci*, **2009**, 2, 872-877.
[23] N. Venkatachalam, M. Palanichamy, V. Murugesan, *J. Mol. Catal. A: Chem.* **2007**, 273, 177-185.
[24] J. Tao, Y. Shen, F. Gu, J. Zhu, J. Zhang, *J. Mater. Sci. Technol,* **2007**, 23, 513-516.
[25] G.S. Shao, X.J. Zhang, Z.Y. Yuan, *Appl. Catal. Environ*, **2008**, 82, 208-218.

[26] W. Lin, Y.F. Zhang, Y. Li, K.N, Ding, J.Q. Li, Y.J. Xu, *J. Chem. Phys*, **2006**, 124(5), 054704-054712.
[27] V. Shklover, M.-K. Nazeeruddin, S.M. Zakeeruddin, C. Barbe, A. Kay, T. Haibach, W. Steurer, R. Hermann, H.-U. Nissen, M. Gratzel, *Chem. Mater*,**1997**, 9, 430-439.
[28] R. Ma, T. Sasaki, Y. Bando. *J. Am. Chem. Socm*, **2004**, 126, 10382-10388.

AUTHORS' ADDRESSES

1. **P.Babji**
Department of Physical, Nuclear Chemistry & Chemical Oceanography,
School of Chemistry,
Andhra University, Visakhapatnam-530 003.
Email: babjichemistry007@gmail.com
Mobile No: 8099852007.
2. **Dr.I.Nageswara Rao**
UGC-Research Scientist-C, Department of Physical, Nuclear Chemistry & Chemical Oceanography,
School of Chemistry,
Andhra University, Visakhapatnam-530 003.
Email: inrao25@yahoo.co.in
Mobile No: 9849286977.